Title
An animal model of SARS produced by infection of Macaca mulatta with SARS coronavirus.

Journal
The Journal of pathology, 206(3)

ISSN
0022-3417

Authors
Qin, Chuan
Wang, Jianwei
Wei, Qiang
et al.

Publication Date
2005-07-01

DOI
10.1002/path.1769

Peer reviewed

Journal of Pathology
J Pathol 2005; **206**: 251–259
Published online 10 May 2005 in Wiley InterScience (www.interscience.wiley.com). **DOI:** 10.1002/path.1769

Original Paper

An animal model of SARS produced by infection of *Macaca mulatta* with SARS coronavirus

Chuan Qin,[1] Jianwei Wang,[2] Qiang Wei,[1] Mingpeng She,[3] Wayne A Marasco,[4] Hong Jiang,[1] Xinming Tu,[1] Hua Zhu,[1] Lili Ren,[2] Hong Gao,[1] Li Guo,[2] Lan Huang,[1] Renquan Yang,[2] Zhe Cong,[1] Lan Guo,[2] Yanbin Wang,[2] Yali Liu,[1] Yili Sun,[2] Shumin Duan,[2] Jianguo Qu,[2] Liangbiao Chen,[2] Wei Tong,[1] Li Ruan,[2] Peimao Liu,[3] Hua Zhang,[3] Jianmin Zhang,[3] Huiyuan Zhang,[3] Depei Liu,[3] Qian Liu,[3] Tao Hong[1,2,3] and Wei He[3]*

[1]*Institute of Laboratory Animal Science, Chinese Academy of Medical Sciences (CAMS) and Peking Union Medical College (PUMC), Beijing, China, 100021*
[2]*Institute of Virology, Chinese Centre for Disease Control and Prevention (CDC), Beijing, China, 100052*
[3]*Institute of Basic Medical Sciences, Chinese Academy of Medical Sciences (CAMS) and Peking Union Medical College (PUMC), Beijing, China, 100005*
[4]*Department of Cancer Immunology and AIDS, Dana-Farber Cancer Institute, Harvard Medical School, Boston, MA 02115, USA*

Correspondence to: Wei He, Department of Immunology, Institute of Basic Medical Sciences, Chinese Academy of Medical Sciences (CAMS) and Peking Union Medical College (PUMC), 5 Dong Dan San Tiao, Beijing, China, 100005. E-mail: heweiimu@public.bta.net.cn

Received: 4 August 2004
Revised: 21 December 2004
Accepted: 8 February 2005

Abstract

A new SARS animal model was established by inoculating SARS coronavirus (SARS-CoV) into rhesus macaques (*Macaca mulatta*) through the nasal cavity. Pathological pulmonary changes were successively detected on days 5–60 after virus inoculation. All eight animals showed a transient fever 2–3 days after inoculation. Immunological, molecular biological, and pathological studies support the establishment of this SARS animal model. Firstly, SARS-CoV-specific IgGs were detected in the sera of macaques from 11 to 60 days after inoculation. Secondly, SARS-CoV RNA could be detected in pharyngeal swab samples using nested RT-PCR in all infected animals from 5 days after virus inoculation. Finally, histopathological changes of interstitial pneumonia were found in the lungs during the 60 days after viral inoculation: these changes were less marked at later time points, indicating that an active healing process together with resolution of an acute inflammatory response was taking place in these animals. This animal model should provide insight into the mechanisms of SARS-CoV-related pulmonary disease and greatly facilitate the development of vaccines and therapeutics against SARS.

Keywords: SARS; coronavirus; animal model; pathology; rhesus monkey

Introduction

SARS is a newly emerging and highly communicable infectious disease of humans that was first detected in South China in November 2002 and then spread globally. Much has been learned about this syndrome, including the epidemiology and transmissibility of SARS-CoV infections and the clinical manifestations of disease [1–6]. Resurgence of SARS remains a distinct possibility in the post-outbreak period [7]. There is therefore an urgent need to establish a reliable animal model for understanding the pathogenesis of SARS-CoV infection and for developing vaccines and antiviral drugs for the prevention and treatment of SARS.

Cynomolgus macaques (*Macaca fascicularis*) [7,8], ferrets (*Mustela furo*), and domestic cats (*Felis domesticus*) are susceptible to infection by SARS-CoV [9,10]. Replication of SARS-CoV in the respiratory tract of mice has also been recently demonstrated [11]. However, the long-term sequelae of SARS-CoV infection with respect to progression of the histopathological changes, the degree of immunological reaction, and the duration of virus replication in these animal models are largely unknown. Given the importance of developing a non-human primate model for elucidating the pathophysiological mechanisms of lung injury and developing new treatments for SARS, we investigated the susceptibility of rhesus macaques (*Macaca mulatta*) to SARS-CoV infection through nasal cavity inoculation. The pathological changes in lungs and other organs after SARS-CoV-inoculation, the replication and excretion of SARS-CoV *in vivo*, and the immune response specific for SARS-CoV in all macaques were studied at different times after virus infection. In this paper, we report our findings on the molecular detection of SARS-CoV replication *in vivo*, the timing of seroconversion and development of neutralizing antibody response, and the dynamic pathological changes in the lungs of infected animals over a 60-day period.

Materials and methods

Animals

All macaques, aged 1–3 years, were obtained from the Institute of Medical Biology (Kunming, China), CAMS and PUMC, and numbered as 1951, 2372, 0227, 1924, 1921, 900, 883, and 2373. Before inoculation with SARS virus, the monkeys were examined according to the national microbiological and parasite SPF (specific pathogen-free) standard and were verified free of anti-SARS antibody. The experiments were performed in BL-3 level laboratories exclusively assigned for SCV research at the Institute of Laboratory Animal Science of CAMS, with an animal study protocol approved by the Institutional Animal Welfare Committee. The macaques were sacrificed according to the study design described in Table 1. This design was the result of a preliminary experiment with four rhesus monkeys sacrificed on the fourth, eighth, 12th, and 16th day post-infection. This experiment showed that the lung lesions were much worse in two monkeys, ie 4 and 8 days after inoculation, and the inflammatory response still persisted on the 16th day post-inoculation. On the basis of these data and the autopsy findings of human SARS patients, monkeys prepared for this experiment were examined on the fifth, tenth, 15th, 20th, 30th, and 60th day post-infection, with the study design focusing on the behaviour of the acute inflammatory response after virus infection. In addition, the possibility of complications such as emphysema, proliferation of fibrous tissue, lung fibrosis, and pleural adhesion at the later stages (60 days) of infection were examined.

Virus

SARS-CoV strain PUMC01 was isolated from a SARS patient in China and cultured with Vero-E6 cells (Genebank accession No AY350 750). The 11th passage virus was used and its $TCID_{50}$ (tissue culture infectious dose 50) was 10^6 per ml titred on Vero-E6 cells [12]. The virus was not resequenced after the initial isolation and DNA sequencing.

Virus inoculation

In a preliminary experiment, monkeys were infected with 10^3, 10^5, and 10^7 TCID. 10^5 TCID was identified as the optimum dose and was inoculated in a volume of 1 ml (after ten-fold dilution of 10^6 per ml stock) into monkeys 900, 2372, 0227, 883, 2373, 1924, and 1921 by dripping into the nasal cavity. Two millilitres of 10% (w/v) lung tissue lysate from a clinically diagnosed SARS patient infected with SARS-CoV strain PUMC01 was inoculated into monkey 1951 intravenously and via the nasal cavity.

Table 1. Sacrifice design in SARS-CoV-infected *Macaca mulatta*

Macaque identification No	Days after sacrifice
2373	5
1924	7
1951	10
883	15
227	20
1921	30
900	60
2372	60

Observations on clinical signs

The animals were subjected to daily measurement of anal temperature, routine blood assays, and chest radiography.

Nested RT-PCR for SARS-CoV

The pharyngeal swab samples were collected from infected monkeys from the first day after inoculation and were tested for SARS-CoV by nested RT-PCR. RNAs were isolated with TRIZOL (Invitrogen). RT-PCR was performed in 50 µl of reaction volume with 25 mM $MgCl_2$, outer primer pair (5′-GCTGCATTGGTTTGT-TATATCGTTATGC-3′) and (5′-ATACAGAATACAT-AGATTGCTGTTATCC-3′), inner primer pair (5′-TCACTTGCTTCCGTTGAGGT AGCCAGCGTGGT-GGTTCATACAA-3′), and (5′-G GTTTCGGATGTTA-CAGCGTCTCCCGGCAGAAA GCTGTAAGCT-3′). The amplification parameters used were sequentially as follows: outer primer pair: 50 °C, 30 min for reverse transcription, then 30 s at 94 °C, 30 s at 55 °C, and 1 min at 72 °C for 30 cycles, followed by a final extension for 10 min at 72 °C; inner primer pair: 10 min at 37 °C, 10 min at 94 °C; 30 s at 94 °C, 30 s at 60 °C, and 1 min at 72 °C for 32 cycles, followed by a final extension for 10 min at 72 °C. All PCR products were verified by nucleotide sequencing.

Isolation of SARS-CoV

At 2, 5, and 7 days post-infection, the pharyngeal swab samples from the infected macaques were inoculated onto Vero-E6 cells and cultured in DMEM (Gibco, USA). For virus isolation, at least three to four passages of the isolates were carried out on Vero-E6 cells. Both cytopathic effect (CPE) and immunofluorescence assay (IFA) (incubation with 1 : 10 dilution of SARS patient serum) were used to determine the infection status of the animals.

Antibody detection

Just before infection, and on days 5, 9, 13, 17, 20, and so on after virus inoculation, blood samples were collected from each animal for SARS-CoV antibody assay by ELISA (ELISA kit; Huada S20030004, Beijing, China). The plates were coated with cell lysates from SARS-CoV-infected Vero-E6 cells. All samples were run in duplicate and simultaneously incubated at 37 °C for 1 h, washing for six times with PBS-T. Plates were blocked once again for 30 min at

37 °C and washed five times. 100 μl of horseradish peroxidase (HRP)-conjugated mouse anti-monkey IgG (Santa Cruz Biotechnologies, Santa Cruz, CA, USA) was added to the wells and incubated for 1 h at 37 °C and then washed six times with PBS-T, developed with 100 μl of 3,3,5,5-tetramethylbenzidine solution (Roche-Boehringer-Mannheim, Mannheim, Germany), and stopped with 100 μl of 2 M sulphuric acid. Plates were read spectrophotometrically at 450 nm in a microplate reader (Labsystems IEMS, Helsinki, Finland). Samples with OD < 0.16 were considered negative. This cut-off point was determined using serum from a normal rhesus monkey that produced no colour development by immunofluorescence of SARS-CoV-infected Vero cells as a negative control.

To determine neutralization activity, the macaques' serum was serially diluted two-fold from 1 : 2 to 1 : 512 and incubated with 10^2 TCID SARS-CoV for 1 h at 37 °C, and then inoculated onto Vero-E6 cells in a 96-well-plate. Each dilution of serum was tested in three wells. The cells were cultured for 1 week to observe for CPE, and the serum dilution in which 50% of the cells were protected from infection was calculated.

Pathological examination

Autopsies were performed in the biosafety level 3 (BSL3) animal laboratory at different intervals after infection. Organs were grossly examined and tissue blocks were taken from the lungs, hilar lymph nodes, heart, liver, kidneys, intestines, adrenals, thymus, mesentery lymph nodes, and brains. Haematoxylin and eosin (H&E) stain, Verhoeff's stain, periodic acid-Schiff (PAS) stain, Mallory's connective tissue (MCT) stain, phosphotungstic acid haematoxylin (PTHA), and Gomori's stains were used to identify changes in collagen fibres, elastic and reticulin fibres, alveolar lining cells, hyaline membranes, and mucus in the alveolar spaces.

Sections were also stained with monoclonal antibodies (MAbs) for cytokeratin, CD68, and CD35 to identify the origin of different types of macrophages in alveoli and in inter-alveolar septa at different times after virus inoculation. MAbs against CD4 and CD8 were used for T-lymphocyte subset identification.

SARS-CoV antigens were detected in various tissues by immunohistochemical staining. Duplicate sections of all tissue samples were stained using an avidin–biotin complex peroxidase technique. Dewaxed sections were pretreated with protease K (Sigma, St Louis, MO, USA) for 10 min at 37 °C, blocked with 3% hydrogen peroxide and non-immune goat serum for 30 min, and then incubated with MAbs against SARS-CoV (1 : 400) overnight at 4 °C. These antibodies were a gift from Dr Yiyou Chen, Starvax, Inc, Beijing, China and comprised a pool of anti-SARS spike and anti-SARS nucleocapsid MAbs. The slides were developed using biotin-labelled goat anti-mouse antibody according to the manufacturer's recommendations (Beijing Zhongshan Biotech, China).

Electron microscopy

Samples of lung, spleen, and lymph node were fixed in 4% formaldehyde and 1% glutaraldehyde, and post-fixed in 1% osmium tetroxide. Tissue samples were embedded in epoxy resin Epon812. Thin sections were doubly stained with uranyl acetate and lead citrate, and examined under a Tecnai 12 (FEI) transmission electron microscope.

Results

Clinical signs

Two to three days after SARS-CoV inoculation, all eight monkeys showed a temporary rise in temperature that peaked initially at 40 °C, but subsequently subsided to 38 °C. There were no remarkable changes in leukocyte count, and clinical signs and symptoms including cough, upper respiratory tract catarrh, dyspnoea, loss of appetite, vomiting, rash, and diarrhoea were absent. Moreover, chest radiography was negative in all of the experimental monkeys in the early stage after virus inoculation.

Replication and release of virus

SARS coronavirus RNA was detected as a 797 bp fragment by nested RT-PCR in the pharyngeal swab and nasal swab samples from the infected macaques on the first day after infection. Positive results were found in all eight monkeys (Table 2) from the fifth to 16th day post-infection.

Pharyngeal specimens were cultured with Vero cells and showed CPE, suggesting the replication of SARS-CoV. Electron microscopy of Vero cells with CPE demonstrated typical SARS-CoV particles in cell culture supernatant using negative staining. SARS-CoV could also be confirmed by electron microscopy of the necropsy samples from monkeys 1951, 1921, 1924, and 227 (Table 3). Further

Table 2. Experimental results in SARS-CoV-infected *Macaca mulatta*

Macaque identification No	RT-PCR* (days)	Virus isolation† 2/5/7 days	IgG
2373	2–5	+/−/−	−‡
1924	5–7	+/−/−	−‡
1951§	2–10	+/+/−	−‡
883	5–10	−/+/−	+
227	5–11	−/−/−	+
1921	5–9	−/−/−	+
900	1–16	+/−/−	+
2372	5–11	−/−/−	+

* From the fifth day post-infection, nasal and pharyngeal samples from all monkeys were detected as positive; the longest lasted to day 16.
† Virus isolation is positive if any pharyngeal and nasal swab samples collected on days 2, 5, and 7 yield positive results.
‡ *Macaca mulatta* were sacrificed before the tenth day.
§ Inoculated intravenously and via the nasal cavity with lung tissue lysate from a SARS patient.

proof came from immunohistochemical detection in necropsy samples from monkey 1951 at 10 days post-infection (Figure 1).

Immunological responses

The serum samples obtained from all eight animals prior to inoculation were negative for anti-SARS antibodies, but such antibodies were detectable in five of eight infected monkeys from 11 to 60 days post-infection. As shown in Table 4, neutralization assays demonstrated that all tested monkeys were able to produce neutralizing antibody. The titre of neutralizing antibody for each monkey was as follows: No 883, 1 : 4 (15 days post-infection); No 0227, 1 : 2 (20 days post-infection); No 1921, 1 : 4 (30 days post-infection). Both No 900 and No 2372 showed a titre of 1 : 64 (60 days post-infection).

Table 3. Presence of SARS-CoV in tissues of infected *Macaca mulatta* detected by electron microscopy

Macaque identification No (day sacrificed)	Lung	Lymph node	Spleen	Liver	Kidney
1924*(7)	+	+	–	–	–
1951(10)	+	+	+	–	–
227(20)	+	–	–	–	–
1921(30)	+	–	–	–	–

* Inoculated intravenously and via the nasal cavity with lung tissue lysate from a patient infected with SARS-CoV strain PUMC01.

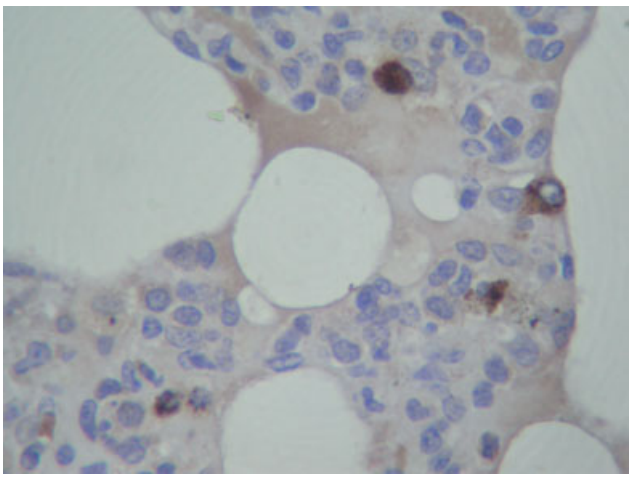

Figure 1. SARS-CoV antigen in lung tissues from infected *Macaca mulatta* (No 1951) 10 days after infection. Lung tissue samples were stained using an avidin–biotin complex peroxidase technique. Sections were incubated with monoclonal antibodies against SARS-CoV (1 : 400) and were developed using biotin-labelled goat anti-mouse antibody. (Immunohistochemical staining; original magnification ×400)

Pathological changes

Lung tissue from healthy rhesus monkeys showed normal alveolar septa, intact reticulin fibres and lining epithelium, with occasional CD68-positive foam cells adherent to regenerating epithelial cells (Figure 3). In striking contrast, lung lesions developed in all eight SARS-CoV-infected monkeys. Grossly, there was congestion, and palpable nodules, scattered in distribution, were located particularly in the posterior part of different lobes (Figure 2). Microscopically, lesions were demonstrated in different organs, particularly in the lungs where acute haemorrhagic interstitial pneumonia (Figures 4A, 4B, 5A, 5B, and 7A) or acute interstitial pneumonia (Figures 4C, 4D, 6C, and 7C) was remarkable.

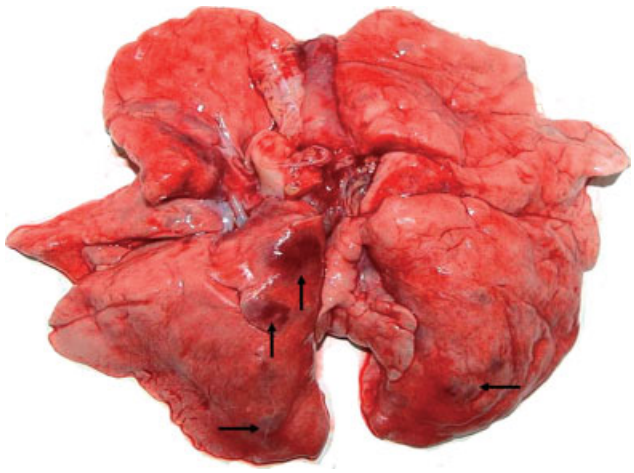

Figure 2. Macroscopic appearance of lung tissue of SARS-CoV-infected monkey 2373 on the fifth day after infection; local lesions are arrowed

Table 4. Changes of IgG and neutralizing antibody titres in sera from SARS-CoV-infected *Macaca mulatta*

Macaque identification No (see Table 1)	0*	5	10	15	20	30	40	50	60
2373	–	–†							
1924	–	–†							
1951	–	–	–†						
883	–	–	–	1 : 40‡ (1 : 4)					
227	–	–	1 : 10	1 : 160	1 : 160 (1 : 2)				
1921	–	–	–	–	–	1 : 40 (1 : 4)			
900	–	–	–	1 : 80	1 : 80	1 : 320	1 : 160	1 : 160	1 : 160 (1 : 64)
2372	–	–	1 : 40	1 : 320	1 : 320	1 : 320	1 : 160	1 : 160	1 : 160 (1 : 64)

* Days after infection with SARS-CoV.
† *Macaca mulatta* were sacrificed on or before the tenth day.
‡ Sera were diluted from 1 : 10. Negative (–) = OD value < 0.16.
Antibody titres were determined on the days when the monkeys were sacrificed and are given in parentheses.

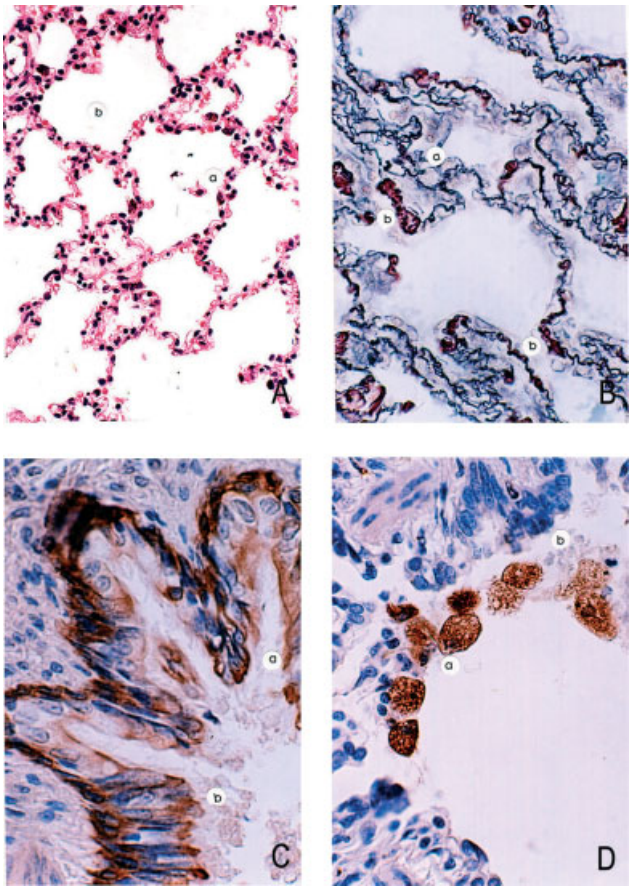

Figure 3

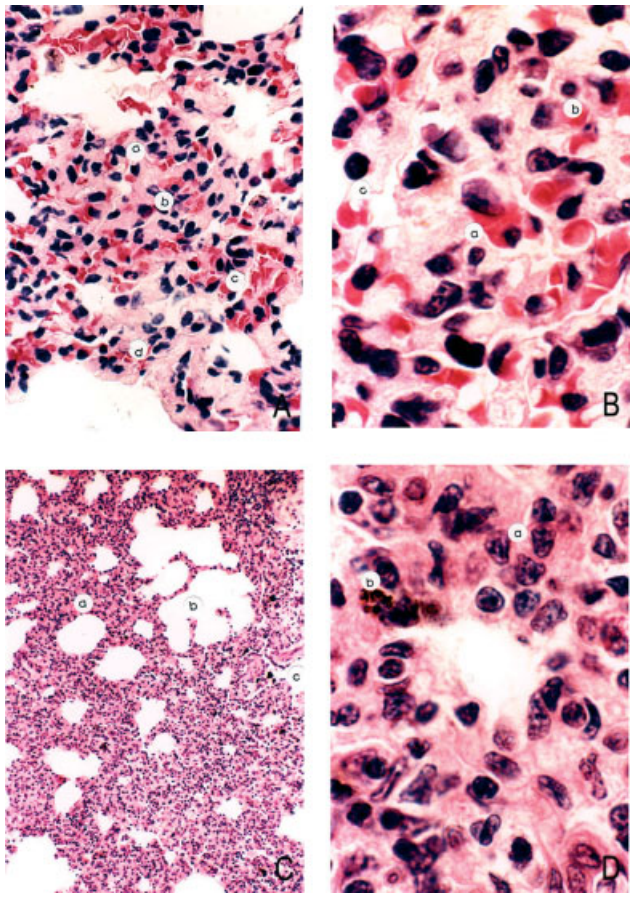

Figure 5

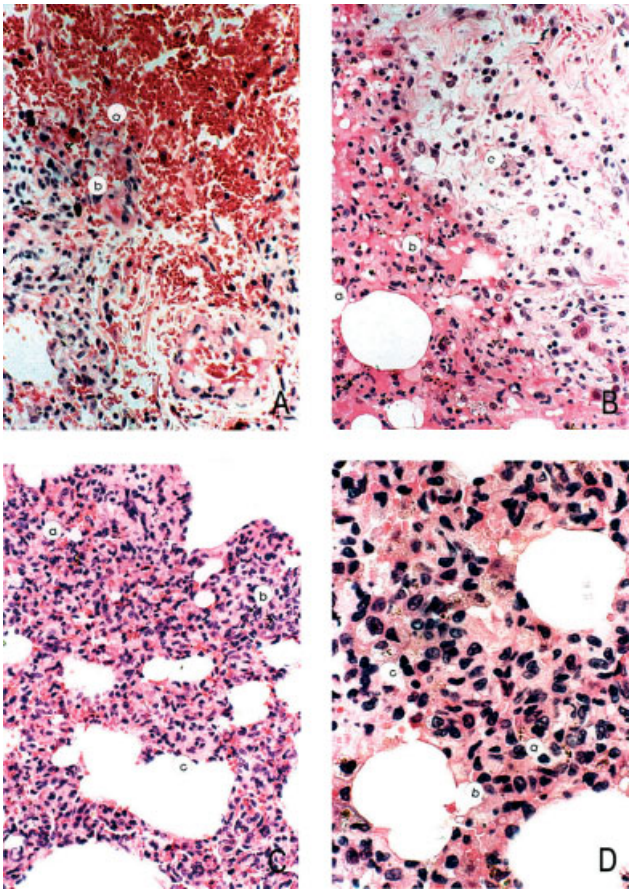

Figure 4

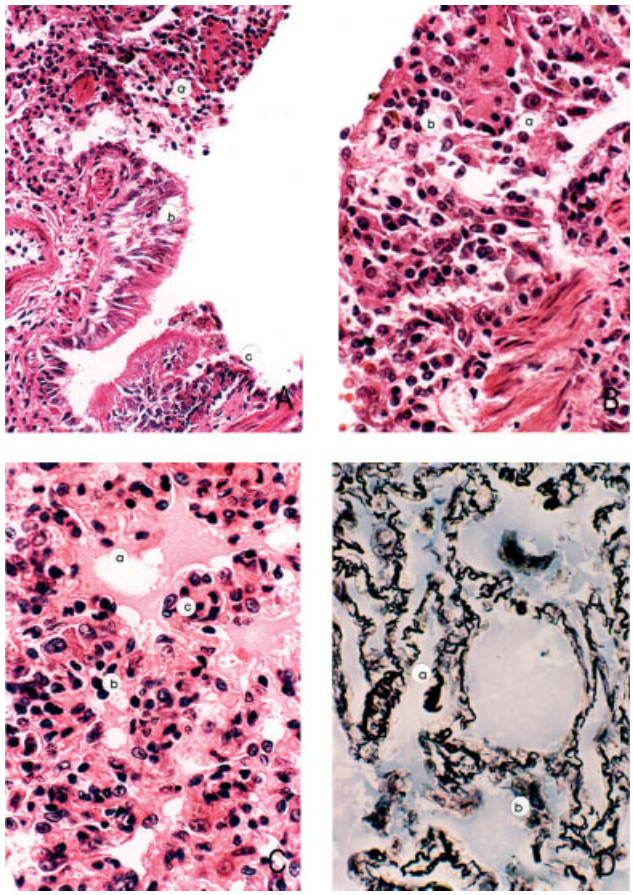

Figure 6

Figure 3. Lung alveoli of a normal healthy rhesus monkey for comparison. (A) Normal alveolar septa (H&E; original magnification ×200). (A, a) The inter-alveolar septa are narrow; there is no inflammatory cell infiltration or oedema (H&E; original magnification ×200). (A, b) The alveolar sacs are clear; no inflammatory cells are seen in any of the alveoli shown (H&E; original magnification ×200). Panel B, a shows intact reticulin fibres in the alveolar septa; B, b shows small capillaries located in the inter-alveolar septa (MCT; original magnification ×400). Panel C shows the intact lining epithelium; C, a, b shows positive staining of epithelial cells with a monoclonal anti-cytokeratin antibody (CK+; original magnification ×1000). Panel D, a, b shows that foam cells staining positive for CD68 are adherent to regenerating epithelial cells (MAb against human CD68; original magnification ×1000)

Figure 4. Monkey 2373, 5 days after infection. (A, a) Interstitial pneumonia with haemorrhage; (A, b) foam cells (macrophages) with engulfed red blood cells in the cytoplasm (H&E; original magnification ×200). (B, a) Interstitial pneumonia: macrophage infiltration is remarkable, with engulfed red blood cells in their cytoplasm; (B, b) lymphocytes and fibrin deposition; (B, c) pleuritis with oedema, phagocyte and lymphocyte infiltration (H&E; original magnification ×200). (C, a) Haemorrhage; (C, b) macrophages; (C, c) lymphocytes and macrophages (H&E; original magnification ×200). (D, a) Macrophages packed in the alveolus; (D, b) lymphocytes; (D, c) foam cells (H&E; original magnification ×400)

Figure 5. Monkey 1924, 7 days after infection. (A, a) Haemorrhage in the inter-alveolar septum; (A, b) engulfed red blood cells in phagocytes; (A, c) alveoli filled with fibrin, inflammatory cells, and red blood cells; (A, d) lung oedema (HE; original magnification ×400). (B, a) Macrophage with engulfed red blood cell; (B, b) foam cells; (B, c) lymphocytes (H&E; original magnification ×1000). (C, a) Interstitial pneumonia; (C, b) distended air sacs; (C, c) dilatation of respiratory duct (H&E; original magnification ×200). (D, a) Macrophages; (D, b) lymphocytes in the inter-alveolar septum (H&E; original magnification ×1000)

Figure 6. Monkey 1951, 10 days after infection. (A, a) Granulation tissue in the damaged bronchiolar wall; (A, b) proliferation of the lining epithelial cells; (A, c) early regeneration of the damaged epithelium (H&E; original magnification ×200). (B, a) Phagocytes; (B, b) lymphocytes (H&E; original magnification ×400). (C, a) Lung oedema; (C, b) interstitial pneumonia; (C, c) foam cells (H&E; original magnification ×400). (D, a) Fragmentation of reticulin fibres in the alveolar wall; (D, b) desquamation of epithelial cells (Gomori's stain; ×1000)

The pathological changes found in the lungs and other organs of monkeys sacrificed at different intervals after viral infection were as follows:

Pathological changes 5 days after virus inoculation (No 2373)

Haemorrhagic interstitial pneumonia (Figures 4A, a, b and 4B, a–c) and interstitial pneumonia (Figures 4C, a–c and 4D, a–c) were observed. Inter-alveolar septa became widened with infiltration of lymphocytes, macrophages, foam cells, and macrophages with engulfed ghost cells (mostly degenerate red blood cells) in the cytoplasm (Figures 4B, a–c and 4D, a–c). The alveolar sacs and a few dilated fine bronchioles were filled with clusters of macrophages.

Pathological changes 7 days after viral inoculation (No 1924)

Haemorrhagic interstitial pneumonia (Figures 5A and 5C) was accompanied by dilatation of the respiratory ducts (Figure 5C, c) and lung oedema (Figure 5A, d) in the nodular areas of different lobes. Alveolar cavities were packed mainly by macrophages and lymphocytes (Figures 5A, a–c; 5B, a–c; and 5D, a, b). Phagocytosis of erythrocytes was common (Figure 5B, a–c).

Pathological changes 10 days after viral inoculation (No 1951)

Proliferation of epithelial cells or over-excretion of mucus was remarkable in the small bronchioles. There was ulceration, granulation tissue formation, and proliferation of the lining epithelial cells in small bronchioles (Figure 6A, a–c); infiltrating inflammatory cells were mainly macrophages and lymphocytes (Figure 6B, a, b). Oedema of the lungs and lesions of interstitial pneumonia were distinct (Figure 6C, a–c). Gomori's silver staining showed destruction and fragmentation of the reticulin fibres of the alveolar wall (Figure 6D, a, b).

Pathological changes in lungs of macaques 15 days (No 883) and 20 days (No 227) after viral inoculation

In monkey 883, interstitial pneumonia was haemorrhagic in nature (Figure 7A, a–c), with infiltration of macrophages and lymphocytes in inter-alveolar septa (Figures 7A, b, c and 7B, b, c) and necrotic foci in the liver and left heart similar to the lesions reported in human autopsy findings [13,14]. Fibrin deposition was obvious in the alveolar cavities forming part of the hyaline membrane in alveoli (Figures 7B, a, c and 7C, a–c).

Monkey 227 also had remarkable interstitial pneumonia (pneumonitis) in both lungs (Figure 7D). This was haemorrhagic in some areas, similar to that seen in case 883 (Figure 7A, b, c). There was accumulation of macrophages and foam cells in the alveoli (Figure 7D, a).

Pathological changes 30 days after viral inoculation (No 1921)

Interstitial pneumonia was still detectable in monkey 1921 30 days post-infection. The lesions were scattered in distribution, with infiltration of mononuclear inflammatory cells (Figure 8A, a, b) and evidence of chronic pleuritis and emphysema (Figure 8A, b). Most of the infiltrating cells were CD68-positive (Figure 8D, a). The spleen was congested with proliferation of red pulp (data not shown). Focal necrosis

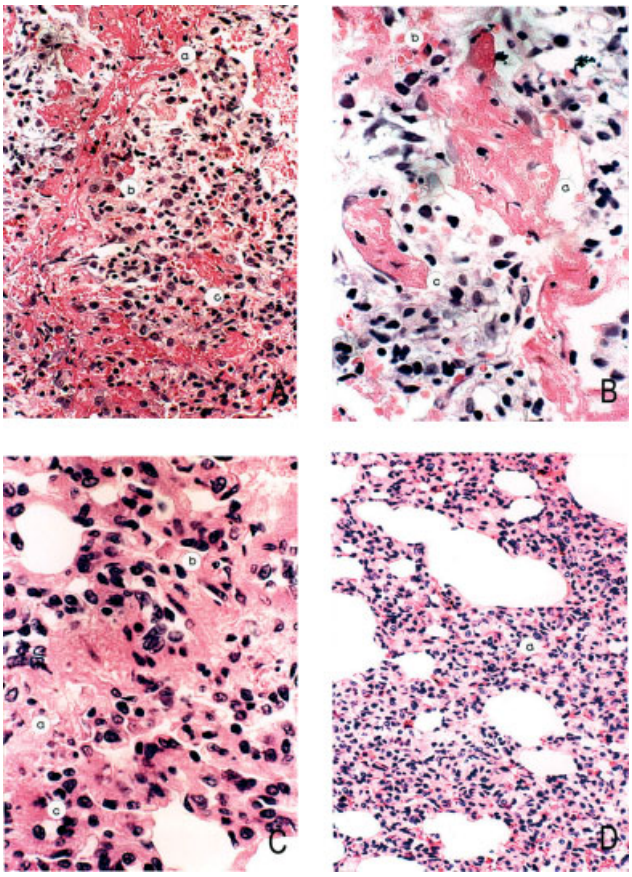

Figure 7

Figure 7. Monkey 883, 15 days after infection. (A, a) Interstitial pneumonia with haemorrhage and fibrin deposition; (A, b) phagocytes with red blood cell engulfment; (A, c) capillary congestion (H&E; original magnification ×200). (B, a) Presence of fibrin filaments between neighbouring alveoli; (B, b) red blood cells engulfed in phagocytes; (B, c) foam cells (H&E; original magnification ×400). (C, a) Lung oedema; (C, b) accumulation of phagocytes in alveoli; (C, c) lymphocytes in the alveolar septum and the alveoli (H&E; original magnification ×400). (D, a) Interstitial pneumonia present in monkey 227

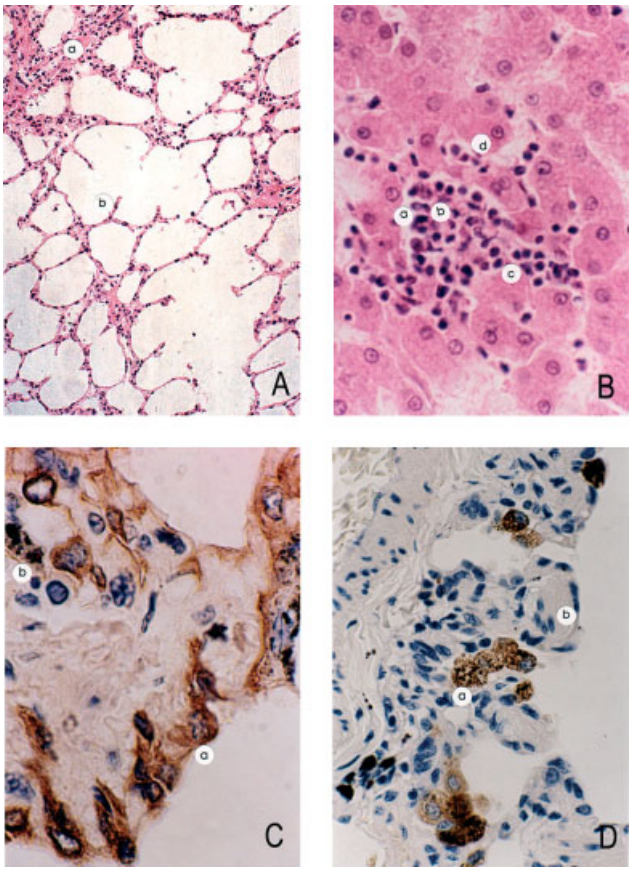

Figure 8

Figure 8. Monkey 1921, 30 days after infection. (A, a) Interstitial pneumonia with mononuclear cell infiltration; (A, b) localized emphysema (H&E; original magnification ×100). (B, a) Focal liver necrosis (No 1921); (B, b) degenerate and necrotic cells; (B, c) lymphocytes; (B, d) liver cells. (C, a) Regenerative epithelial cells shown to be CK-positive (cytokeratin MAb stain; original magnification ×1000); (C, b) macrophages. (D, a) CD68-positive cells (macrophages) adherent to the surface of regenerative epithelial cells (CD68 MAb stain; original magnification ×1000); (D, b) regenerative epithelial cells in small bronchioles

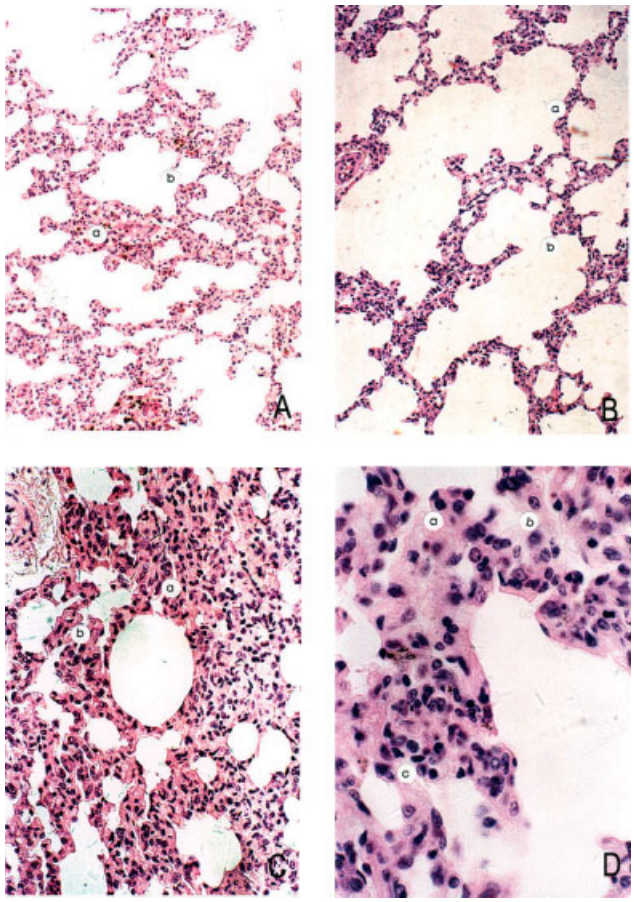

Figure 9. Monkeys 900 and 2372, 60 days after infection. (A, a) Interstitial pneumonia with mononuclear infiltration (H&E; original magnification ×50) (No 2372). (A, b) Some alveoli are distended. (B, a) Mild interstitial pneumonia; (B, b) emphysema (H&E; original magnification ×100) (No 900). (C, a) Interstitial pneumonia and infiltration of mononuclear cells; (C, b) foam cell formation (H&E; original magnification ×200). (D, a) Foam cells in alveoli; (D, b) phagocytes; (D, c) lymphocytes in septa (H&E; original magnification ×400)

was seen in the liver (Figure 8B, a–d). The regenerative epithelial cells of alveoli were cytokeratin-positive (Figure 8C, a, b). Additionally, CD68-positive cells (Figure 8D, a, b) were seen to adhere in clumps to the regenerative epithelial cells of the small bronchioles.

Pathological changes 60 days after viral inoculation (Nos 2372 and 900)

Foci of interstitial pneumonia were still found in certain areas of the lungs in both monkeys but were mild (No 2372, Figure 9A and No 900, Figures 9B–9D). Some alveoli were markedly distended, accompanied by localized emphysema (Figures 9A and 9B). Most of the inter-alveolar septa were well preserved and there was evidence of infiltration of lymphocytes and macrophages in inter-alveolar septa (Figure 9A and monkey 900 in Figures 9C and 9D).

In summary, lesions of acute interstitial pneumonitis were observed in the monkeys throughout the 60-day study. There was marked infiltration of lymphocytes and macrophages in nodular areas in the lungs, particularly in the early stages, ie 5 and 10 days post- infection (Figures 4B, a, b and 4D, a–c; and Figures 5B, a–c and 5D, a, b). Some respiratory ducts were packed with mucus and cell debris and, in addition, regeneration of the lining epithelium was seen simultaneously in certain terminal bronchioles (Figures 6A, a–c and 6B, a, b). Desquamation of alveolar lining cells, lung oedema, and hyaline membranes in alveoli were identified in some infected animals (Figures 6C, a–b; 7B, a, b; 7C, a, b; and 7D, a), however, the lung lesions were less intense compared with the pathological features seen in the lungs of patients who died of SARS [13–15]. The severity of lung infection became mild in those animals that were sacrificed more than 30 days after the infection (Figures 8A, 9B, and 9C). In these animals, there was still infiltration of macrophages and lymphocytes in the inter-alveolar septa (Figure 8A, a, b). Fragmentation of reticulin and elastic fibres of the alveolar wall was common (Figure 6D, a, b). There was also evidence of fibrous tissue proliferation and development of emphysema (Figures 8A and 9B).

Discussion

It is important to establish animal models in order to explore the pathogenesis of SARS and to test new antiviral therapies and vaccines against SARS. In this study, we detected sequential pathological changes in the lungs of macaques from 5–60 days post-infection with SARS-CoV. The pulmonary lesions are comparable to, though less intense than, those of SARS patients. Foci of interstitial pneumonia and diffuse alveolar damage were observed during the whole course of the experiment. Repeated haemorrhage, oedema, and over-secretion of protein-rich fluid inevitably resulted in fibrosis of pulmonary tissues. These pathological changes reflect the changes that are seen in the early stage of clinical SARS cases [16–20]. An important observation in these studies is that there was no SARS-related death in the infected animals and SARS infections in rhesus macaques were milder. The differences in clinical signs and symptoms, and pathological changes, in the experimentally infected rhesus macaques compared with human cases of SARS might be due, in part, to the presence of co-infections or secondary infections in human cases [21,22], whereas the monkeys used in this study were young and healthy. Secondly, treatment given to SARS patients might have had an impact on the histological changes. Thirdly, SARS-CoV might have different cytopathic effects in humans and rhesus macaques.

SARS-CoV-specific IgG antibody could be detected in sera of macaques from 11 days post-infection onwards and the titre increased gradually. Neutralizing antibody protection assays showed that the infected animals produced neutralizing antibodies that could prevent re-infection by SARS-CoV (data not shown). Our results also demonstrate the potent immunogenicity of SARS-CoV, suggesting the possibility of using the virus to produce inactivated or attenuated vaccines.

A recent report has concluded that the macaque model is of limited utility in the study of SARS pathogenesis and the evaluation of therapies [23]. In particular, the lung lesions in both rhesus and cynomolgus macaques were infrequent and limited to focal interstitial alveolar inflammation and oedema and lesions reflecting severe damage to alveolar and bronchial cell damage were not observed. Our results differ from those of Rowe *et al* [23], who showed limited disease, and those of Fouchier *et al* [8] and Kuiken *et al* [24], who showed in cynomolgus macaques a more severe pulmonary syndrome that resembled SARS in several ways. The reasons for these differences are not clear, but it should be noted that rhesus macaques of Chinese origin were used in our studies and viral RNA could be detected in all of the infected monkeys, the longest duration lasting to 16 days. In addition, virus could be isolated from five of eight infected monkeys and neutralizing antibody response persisted in the animals that were sacrificed at 60 days post-infection. Thus, based on the results of virus detection, immunological response, and pathological changes in the lungs of infected animals, we conclude that the rhesus macaque model of SARS is valuable. Furthermore, a long-term study that simultaneously examines the pathological changes and pro-inflammatory cytokine and chemokine profiles in the lungs from these animals might provide insight into the mechanism(s) of SARS-CoV-mediated lung injury and greatly facilitate the screening and evaluation of anti-SARS drugs and vaccines.

Acknowledgements

The present work was sponsored by the National High Technology Research and Development Programme of China

(863 Programme, Nos 2003AA208201, 2003AA208205, and 2003AA208213), the National Nature Science Foundation (No 30340026), the National Institutes of Health (AI-061318), as well as the National Basic Research Programme of China (No 2003CB514109). We are grateful to Mr Wei Deng, Ms Linlin Bao, Ms Yangqi Zhang, and Mr Qi Kong for their excellent technical assistance. We also acknowledge Dr Huiyuan Luo and Dr Qinmin Zhan for reviewing the text. Additional financial support came form the Government of Spain and Mitsui & Co.

References

1. Marra MA, Jones SJ, Astell CR, *et al*. The genome sequence of the SARS-associated coronavirus. *Science* 2003;**300**:1399–1404.
2. Drosten C, Gunther S, Preiser W, *et al*. Identification of a novel coronavirus in patients with severe acute respiratory syndrome. *N Engl J Med* 2003;**348**:1967–1976.
3. Ksiazek TG, Erdman D, Goldsmith CS, *et al*. A novel coronavirus associated with severe acute respiratory syndrome. *N Engl J Med* 2003;**348**:1953–1966.
4. Calza L, Manfredi R, Verucchi G, *et al*. SARS: a new emergency in the world health. *Recent Prog Med* 2003;**94**:284–294.
5. Chiu RW, Chim SS, Lo YM. Molecular epidemiology of SARS — from Amoy Gardens to Taiwan. *N Engl J Med* 2003;**349**:1875–1876.
6. Demmler GJ, Ligon BL. Severe acute respiratory syndrome (SARS): a review of the history, epidemiology, prevention, and concerns for the future. *Semin Pediatr Infect Dis* 2003;**14**:240–244.
7. Enserink M. SARS in China. The big question now: will it be back? *Science* 2003;**301**:299.
8. Fouchier RA, Kuiken T, Schutten M, *et al*. Aetiology: Koch's postulates fulfilled for SARS virus. *Nature* 2003;**423**:240.
9. Martina BE, Haagmans BL, Kuiken T, *et al*. Virology: SARS virus infection of cats and ferrets. *Nature* 2003;**425**:915.
10. Enserink M. Infectious diseases. SARS researchers report new animal models. *Science* 2003;**302**:213.
11. Subbarao K, McAuliffe J, Vogel L, *et al*. Prior infection and passive transfer of neutralizing antibody prevent replication of severe acute respiratory syndrome coronavirus in the respiratory tract of mice. *J Virol* 2004;**78**:3572–3577.
12. Zou K, Zhu H, Ding KY, *et al*. Analysis on the SARS-CoV genome of PUMC01 isolate. *Zhongguo Yi Xue Ke Xue Yuan Xue Bao* 2003;**25**:495–498.
13. Chen YY, Zheng J, Wang RL, *et al*. Pathology changes of severe acute respiratory syndrome (SARS). *Zhonghua Bing Li Xue Za Zhi* 2003;**32**:279–281.
14. Chen J, Zhang HT, Xie YQ, *et al*. Morphological study of severe acute respiratory syndrome (SARS). *Zhonghua Bing Li Xue Za Zhi* 2003;**32**:516–520.
15. Ding YQ, Wang HJ, Shen H, *et al*. Study on etiology and pathology of severe acute respiratory syndrome. *Zhonghua Bing Li Xue Za Zhi* 2003;**32**:195–200.
16. Franks TJ, Chong PY, Chui P, *et al*. Lung pathology of severe acute respiratory syndrome (SARS): a study of 8 autopsy cases from Singapore. *Hum Pathol* 2003;**34**:743–748.
17. Gao ZC, Zhu JH, Sun Y, *et al*. Clinical investigation of outbreak of nosocomial severe acute respiratory syndrome. *Zhongguo Wei Zhong Bing Ji Jiu Yi Xue* 2003;**15**:332–335.
18. Nicholls JM, Poon LL, Lee KC, *et al*. Lung pathology of fatal severe acute respiratory syndrome. *Lancet* 2003;**361**:1773–1778.
19. Ding Y, Wang H, Shen H, *et al*. The clinical pathology of severe acute respiratory syndrome (SARS): a report from China. *J Pathol* 2003;**200**:282–289.
20. Lai RQ, Feng XD, Wang ZC, *et al*. Pathological and ultramicrostructural changes of tissues in a patient with severe acute respiratory syndrome. *Zhonghua Bing Li Xue Za Zhi* 2003;**32**:205–208.
21. Chan PK, Tam JS, Lam CW, *et al*. Human metapneumovirus detection in patients with severe acute respiratory syndrome. *Emerg Infect Dis* 2003;**9**:1058–1063.
22. Poutanen SM, Low DE, Henry B, *et al*. Identification of severe acute respiratory syndrome in Canada. *N Engl J Med* 2003;**348**:1995–2005.
23. Rowe T, Gao G, Hogan RJ, *et al*. Macaque model for severe acute respiratory syndrome. *J Virol* 2004;**78**:11 401–11 404.
24. Kuiken T, Fouchier RA, Schutten M, *et al*. Newly discovered coronavirus as the primary case of severe acute respiratory syndrome. *Lancet* 2003;**362**:263–270.